

FINAL TECHNICAL REPORT

Project Title: Predicting Pattern Tooling and Casting Dimension for Investment Casting

DOE Award Number: DE-FC36-04GO14230

Project Period: July 1, 2007 – July 1, 2008

Date of Report: November 21, 2008

Principal Investigators: Nick Cannell (buyCASTINGS.com)
937.272.2709
ncannell@buyCASTINGS.com

Dr. Mark Samonds, Adi Sholapurwalla, Sam Scott (ESI)
248.203.0642
Mark.Samonds@esi-group.com
Adi.Sholapurwalla@esi-group-na.com
Sam.Scott@esi-group-na.com

Recipient Organization: ESI Group NA
36800 Woodward Avenue
Bloomfield Hills, MI 48304
248.203.0642

Acknowledgment

This report is based upon work supported by the U.S. Department of Energy under award No. DE-FC36-04GO14230. The author wishes to thank the Steel Founders Society of America and the member companies that contributed material and in-kind contributions to this project, without which this research could not have been conducted.

Disclaimer

Any findings, opinions, and conclusions expressed in this report are those of the author and do not necessarily reflect the views of the Department of Energy.

Proprietary Data Notice

This report does not contain any proprietary data.

Report Availability

Reports are available free via the U.S. Department of Energy (DOE) Information Bridge Website:
<http://www.osti.gov/bridge>

Reports are available to DOE employees, DOE contractors, Energy Technology Data Exchange (ETDE) representatives, and Informational Nuclear Information System (INIS) representatives from the following source:

Office of Scientific and Technical Information
P.O. Box 62
Oak Ridge, TN 37831
Tel: (865) 576-8401
FAX: (865) 576-5728
E-mail: reports@osti.gov
Website: <http://www.osti.gov/contract>

Contents

1.	List of Figures.....	4
2.	Abbreviations, Acronyms and Symbols.....	5
3.	Executive Summary.....	6
4.	Introduction.....	7
5.	Approach.....	8
5.1.	Wax Material Property Determination.....	8
5.2.	Software Implementation of Material Property Data.....	9
5.3.	Validation with Experimental Results.....	12
6.	Results of Step Block Analysis.....	15
6.1.	Comparison of Analytical Result to Experimental Data.....	25
7.	Benefits Assessment.....	29
8.	Commercialization.....	29
9.	Conclusion.....	30
10.	Recommendations.....	31
11.	References.....	32
12.	Appendix A.....	33

1. List of Figures

1.	PreCAST GUI Displaying Cerita 29-51 Modulus of Elasticity.....	9
2.	Poisson's Ratio & Coefficient of Thermal Expansion of Cerita 29-51.....	10
3.	Shear Modulus Constant & Relaxation Parameters of Cerita 29-51	10
4.	Conductivity of Cerita 29-51.....	11
5.	Density of Cerita 29-51	11
6.	Specific Heat of Cerita 29-51	12
7.	Step Block Test Geometry.....	13
8.	Isochron to Final Temperature (28.1 C).....	15
9.	Effective Stress After 2 Minutes.....	16
10.	Effective Stress After 4 Minutes.....	16
11.	Effective Stress After 6 Minutes.....	17
12.	Effective Stress After 8 Minutes.....	17
13.	Effective Stress After 10 Minutes.....	18
14.	Effective Stress – Final State.....	18
15.	Principal Stress After 2 Minutes.....	19
16.	Principal Stress After 4 Minutes.....	20
17.	Principal Stress After 6 Minutes.....	20
18.	Principal Stress After 8 Minutes.....	21
19.	Principal Stress After 10 Minutes.....	21
20.	Principal Stress – Final State.....	22
21.	Final Deformed Wax Part (Magnified 10x).....	23
22.	Final Deformed Wax Part (Magnified 10x).....	23
23.	X-Displacement (Values Relative to Original Position)	24
24.	Y-Displacement (Values Relative to Original Position)	24
25.	Z-Displacement (Values Relative to Original Position).....	25
26.	Shrinkage Along Test Part Length (X-Direction)	26
27.	Shrinkage Along Test Part Width (Y-Direction).....	27
28.	Shrinkage Along Test Part Height (Z-Direction).....	28

2. Abbreviations, Acronyms, Symbols

ORNL – Oak Ridge National Lab

DMA – dynamical mechanical analysis

GUI – graphical user interface

C – Celcius / Centigrade

F – Fahrenheit

MPa – mega-Pascal

mm - millimeter

3. Executive Summary

The investment casting process is an expendable mold process where wax patterns of the part and rigging are molded, assembled, shelled and melted to produce a ceramic mold matching the shape of the component to be cast. Investment casting is an important manufacturing method for critical parts because of the ability to maintain dimensional shape and tolerances. However, these tolerances can be easily exceeded if the molding components do not maintain their individual shapes well.

In the investment casting process there are several opportunities for the final casting shape to not maintain the intended size and shape, such as shrinkage of the wax in the injection tool, the modification of the shape during shell heating, and with the thermal shrink and distortion in the casting process.

Studies have been completed to look at the casting and shell distortions through the process in earlier phases of this project. Dr. Adrian Sabau at Oak Ridge National Labs performed characterizations and validations of 17-4 PH stainless steel in primarily fused silica shell systems with good agreement between analysis results and experimental data. Further tasks provided material property measurements of wax and methodology for employing a viscoelastic definition of wax materials into software.

The final set of tasks involved the implementation of the findings into the commercial casting analysis software ProCAST, owned and maintained by ESI Group. This included:

- the transfer of the wax material property data from its raw form into separate temperature-dependent thermophysical and mechanical property datasets
- adding this wax material property data into an easily viewable and modifiable user interface within the pre-processing application of the ProCAST suite, namely PreCAST
- and validating the data and viscoelastic wax model with respect to experimental results

4. Introduction

The investment casting process is an expendable mold process where wax patterns of the part and rigging are molded, assembled, shelled and melted to produce a ceramic mold matching the shape of the component to be cast. A hallmark and primary reason investment casting is selected as the manufacturing method of critical parts comes from the process' ability to maintain dimensional shape and tolerances. However, these tolerances can be easily exceeded if the molding components do not maintain their individual shapes well.

Backtracking through the process, the heated shell must be of a size to produce the proper final shape. The heated shell cavity dimensions come from the firing and dewaxing of the cold shell formed around wax components. The wax components are a product of wax injection into a tool. Therefore from the shrinkage of the wax in the injection tool to the modification of the shape during shell heating and finally with the thermal shrink and distortion in the casting process, there are several opportunities for the final casting shape to not maintain the intended size and shape.

Studies have been completed to look at the casting and shell distortions through the process in earlier phases of this project. Dr. Adrian Sabau performed characterizations and validations of 17-4 PH stainless steel in primarily fused silica shell systems with good agreement between analysis results and experimental data. Further tasks in the project provided material property measurements of wax and methodology for employing a viscoelastic definition of wax materials into software.

The final set of tasks in this project revolves around the implementation of these developments into the commercial casting analysis software ProCAST, owned and maintained by ESI Group. ESI will transfer the wax material property data from its raw form into separate temperature-dependent thermophysical and mechanical property datasets; add this wax material property data into an easily viewable and modifiable user interface within the pre-processing application of the ProCAST suite, namely PreCAST; and validate the data and viscoelastic wax model with respect to experimental results.

5. Approach

The accepted proposal calls for two separately funded phases to implement the wax data into the viscoelastic calculation provided in the ProCAST Stress module. The first phase works with the “unfilled” wax data provided in previous work by Oak Ridge National Lab (ORNL), and is tasked as follows:

Gather all the relevant information on the unfilled wax model from ORNL.

Transfer this material data into ProCAST pre-processor so that users do not have to hard wire this information to run the wax model in the casting simulation program.

Validate the datasets from PreCAST (pre-processor of ProCAST) so that all the material property information is available in graphical format.

Validate wax model using the test geometry with respect to experimental results.

The key components of this phase are the transfer of material data and validation of the wax model with experimental results. The transfer of material data requires converting the data from its raw form into a form which can be used and understood by the viscoelastic algorithm. As noted in previous project reports by Sabau, the data provided by wax suppliers is not sufficient for performing a full thermal and stress calculation. Therefore, the full set of required thermo-physical and mechanical data was gathered. Once the material property data is implemented into the software, a trial will be performed, where the wax solidification and deformation process is simulated with final dimensional results compared to experimental data of the same process.

5.1 Wax Material Property Determination

As noted, the wax material properties commonly determined and distributed by wax suppliers is limited in the thermophysical and mechanical property definitions. This information typically contains information on the melting of the wax and some basic data related to the fluidity of the wax. However, this data is not detailed enough to provide accurate simulation results and fully characterize the material. Additionally, mechanical information is not typically provided to characterize the viscoelastic nature of wax.

Therefore, one of the tasks leading up to this project was the determination of these various material properties. This work was overseen by Dr. Adrian Sabau, where the unfilled wax “Cerita 29-51”, produced and supplied by Argueso, was fully characterized by various laboratory measurements. Full information on the characterization techniques and data may be found in the resulting paper by Sabau and Viswanathan¹. While typical thermophysical data was gathered in traditional methods, a more complex technique was required to get the mechanical shear modulus characterization of the wax, as the viscoelastic behavior of the material must be observed over a large time and temperature range.

To gather the property data over these dual domains, the principle of “time-temperature superposition” is employed, which is defined in the Sabau and Viswanathan² paper as “that time and temperature have an equivalent influence on the viscoelastic properties of

polymers; an increase in temperature corresponds to an extension of the time scale of the experiment.” The data was obtained using dynamical mechanical analysis (DMA) measurements. These stress-strain tests are performed across a range of frequencies and at different temperatures and results in segments of the modulus definition across a frequency range, where each segment corresponds to the temperature of the test. The superposition principle is then applied which shifts these segments along the frequency scale until a continuous curve of modulus is formed. This curve is termed the “master curve”. The last step of the conversion of DMA measurements to a usable form of material property is to convert this modulus information from a “frequency-dependent” definition to a “time-dependent definition”, which specifies the time effect on the mechanical properties. This requires determining the relation times and strengths, which are found via non-linear regression of the master curve.

5.2 Software Implementation of Material Property Data

As the material property data is now in terms of the characterized equations used to calculate the various thermal and mechanical phenomenon experienced in the solidification and deformation of wax injection, the data can be entered into the software and made available to the user. In the pre-processor of the ProCAST suite, PreCAST, forms were created to allow viewing and modification of pure viscoelastic mechanical definitions. Additionally, the material information for the Cerita 29-51 was coded into the material database of the software and made part of the default installation of ProCAST for all users. This implementation can be seen in Figures 1-6, below, where screenshots of the database entry for this material are presented.

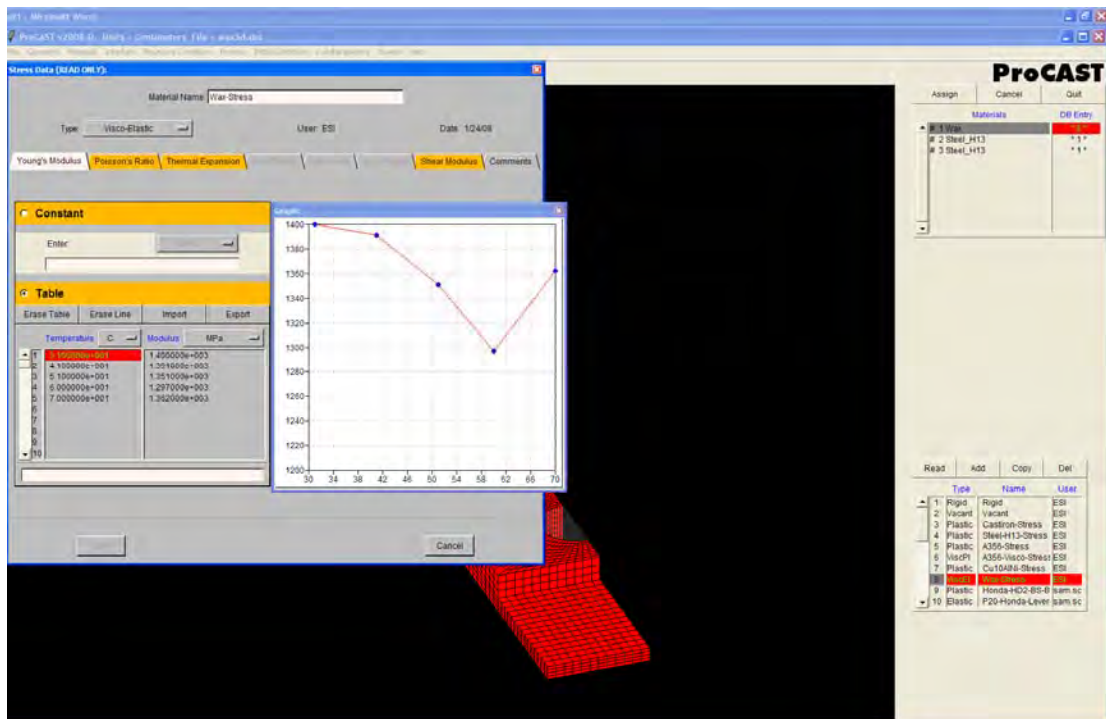


Figure 1 – PreCAST GUI Displaying Cerita 29-51 Modulus of Elasticity

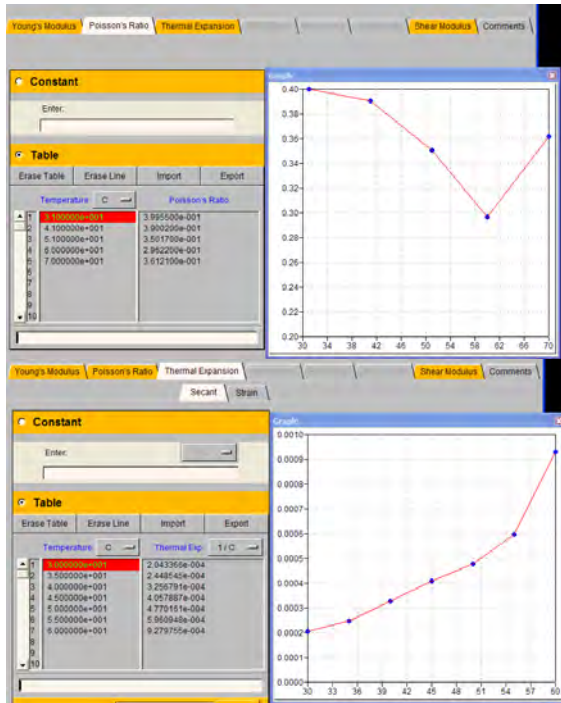


Figure 2 – Poisson's Ratio & Coefficient of Thermal Expansion of Cerita 29-51

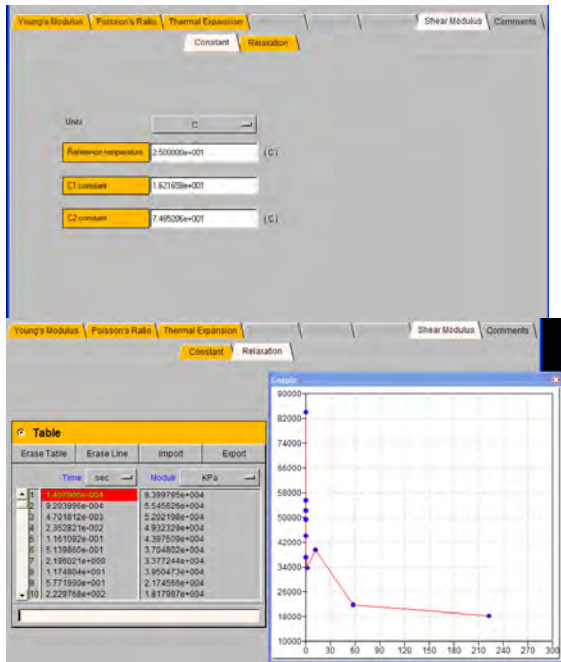


Figure 3 – Shear Modulus Constant & Relaxation Parameters of Cerita 29-51

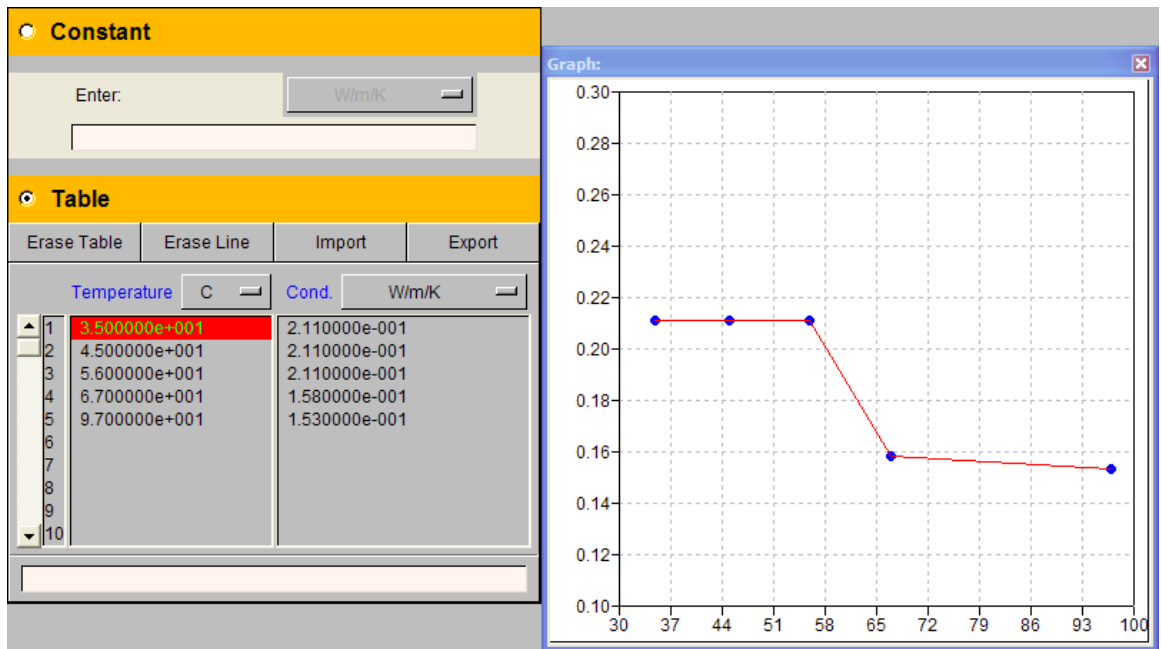


Figure 4 – Conductivity of Cerita 29-51

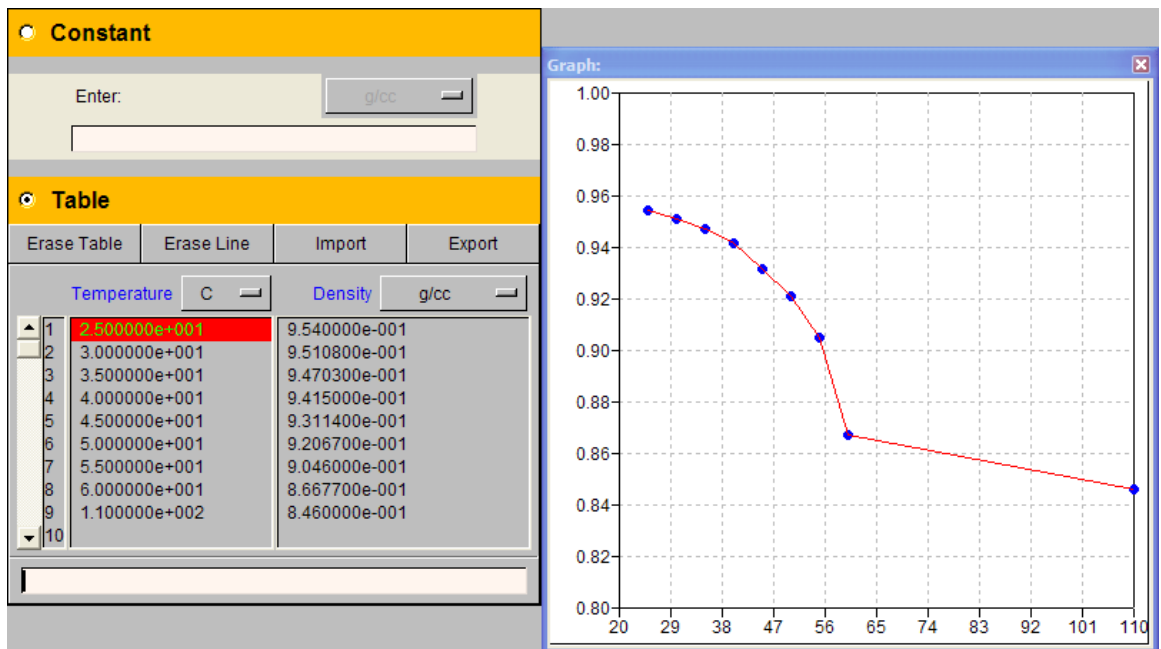


Figure 5 – Density of Cerita 29-51

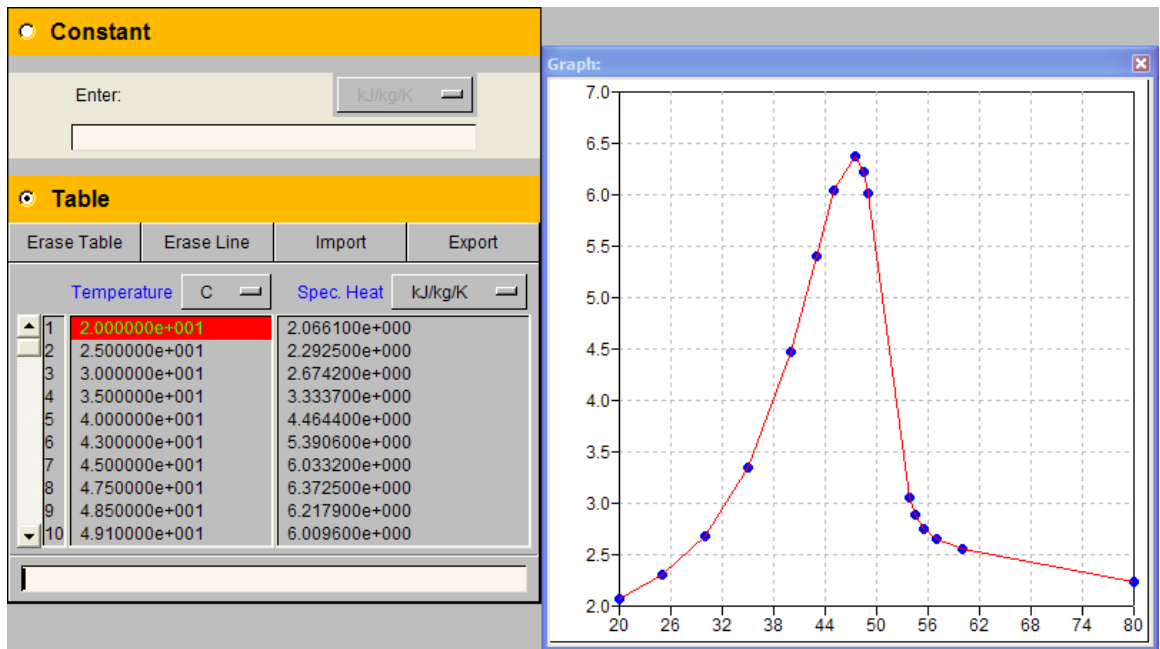


Figure 6 – Specific Heat of Cerita 29-51

5.3 Validation with Experimental Results

The final stage of the Cerita 29-51 implementation is to ensure that the algorithms in the software as well as the material property data are in proper working order. Therefore, a test was prepared where a wax geometry was molded and measured, and a simulation was performed of the same process. The selected test geometry is a wax step block with holes, as displayed in Figure 7.

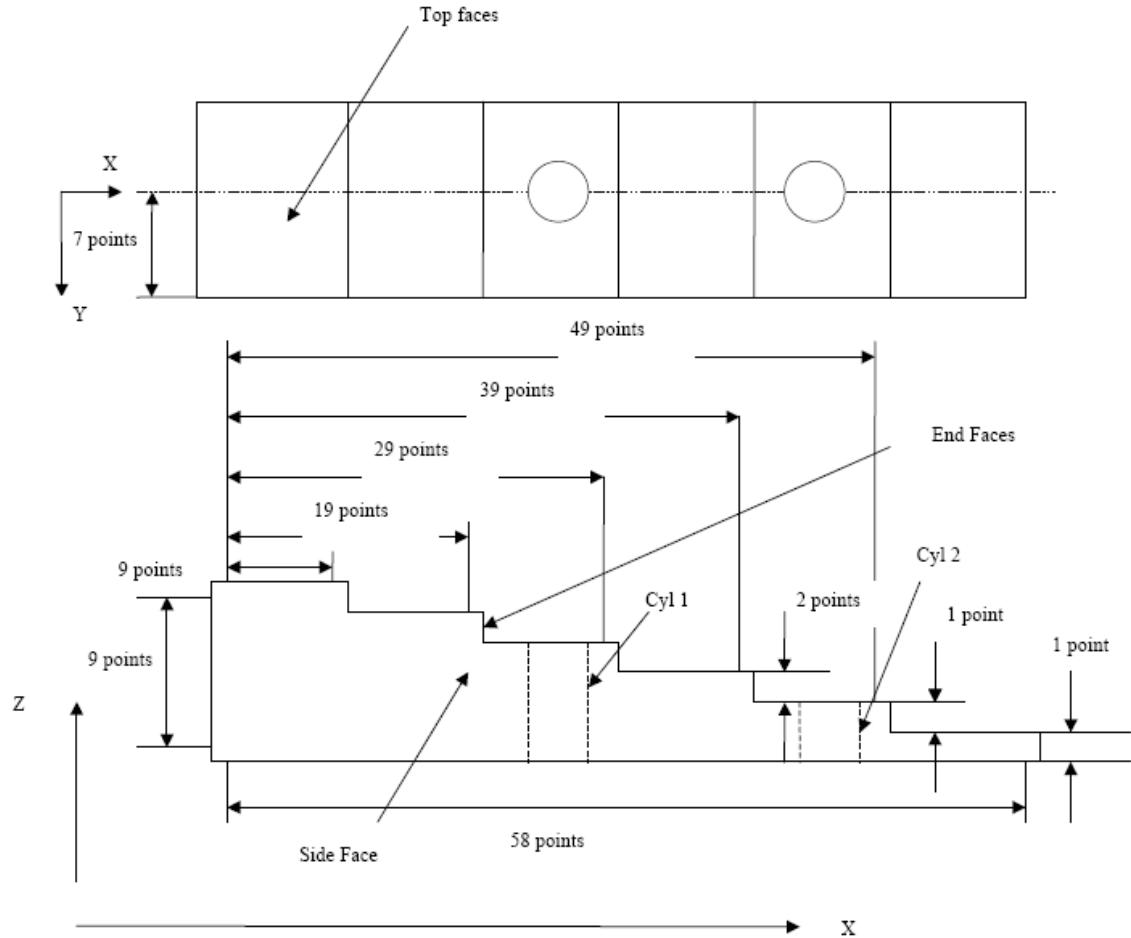


Figure 7 – Step Block Test Geometry

The dimensions of the step block cavity in the wax die are 6.0" long (X-Direction), 1.5" wide (Y-Direction), and each step incrementing 1/6", giving a maximum height of 1.0" (Z-Direction). The holes are centered on the specific individual step faces as shown and are 0.5" in diameter. The dimensions of the manufactured wax, which would have undergone deformation during the process, were gathered using a point measurement device. Equally spaced data points on the sample were collected as noted in the Figure for four samples.

The layouts and measurements for this geometry were done at Oak Ridge National Lab, under the guidance of Dr. Adrian Sabau. Other layouts were provided by Seacast, MCT/Hitchiner and Schrey & Sons.

From the resulting data, wax thicknesses were determined per corresponding data point pair in all three dimensions. These dimensions were individually averaged across all four trial blocks. The results were then plotted in each direction and graphed along the axes of the block.

This step block geometry was then generated in a solid modeling software and meshed in a third party software using linear brick finite elements of a mesh density suitable for accurate calculation of the thermal and stress transients during the process of solidification and cooling of the wax. This mesh was then opened into PreCAST to set up the material property assignments and to define the process on the geometry. As the focus of both the material data gathering and analysis are on the solidification of the wax, the simulation analyzed the solidification and cooling of the wax from an initial uniform temperature of 54.4 C down to 28 C. This cooling was supplied by a Heat Condition on the exterior of the wax, with a film coefficient of 200 W/m²/K, and an ambient temperature of 28 C. As the holes were also meshed, material properties of H-13 steel were assigned to these holes, and an interfacial heat transfer coefficient of 100 W/m²/K was assigned. These steel posts were assumed to be rigid: non-moving and non-deforming. Finally, to fully constrain the part, the flat bottom of the step block (XY-Plane) was set to not move in the Z-direction. As the part is symmetric along the width, one-half of the model was used in this direction.

6. Results of Step Block Analysis

The complete cooling of the part occurred in 3400 seconds, or approximately 57 minutes. The fastest region to cool was the thinnest step, while the center of the thickest two steps took the longest (Figure 8). This plot also indicates that in the thicker sections, the cooling started at the exterior surfaces and moved inward. Therefore, the softest and weakest material was formed at the center of the wax. This may be compensated by the wax intensification, which is not within the scope of this project.

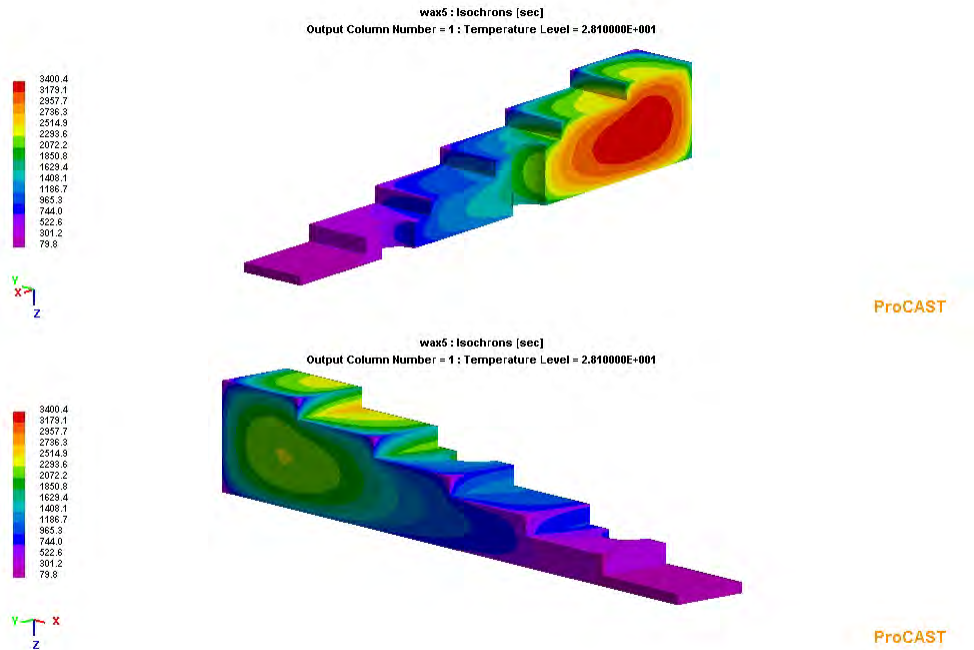


Figure 8 – Isochron to Final Temperature (28.1 C)

This cooling pattern creates stresses in the wax, with further stresses formed by the holes providing a constraint against shrinking along the block primarily in the X-direction, and a small amount of shrink prevention in the Y-direction local to the posts. The combination of cooling pattern and constraints form the effective stresses as shown in Figures 9 through 14, which present the evolution and final state of the effective stresses in the wax.

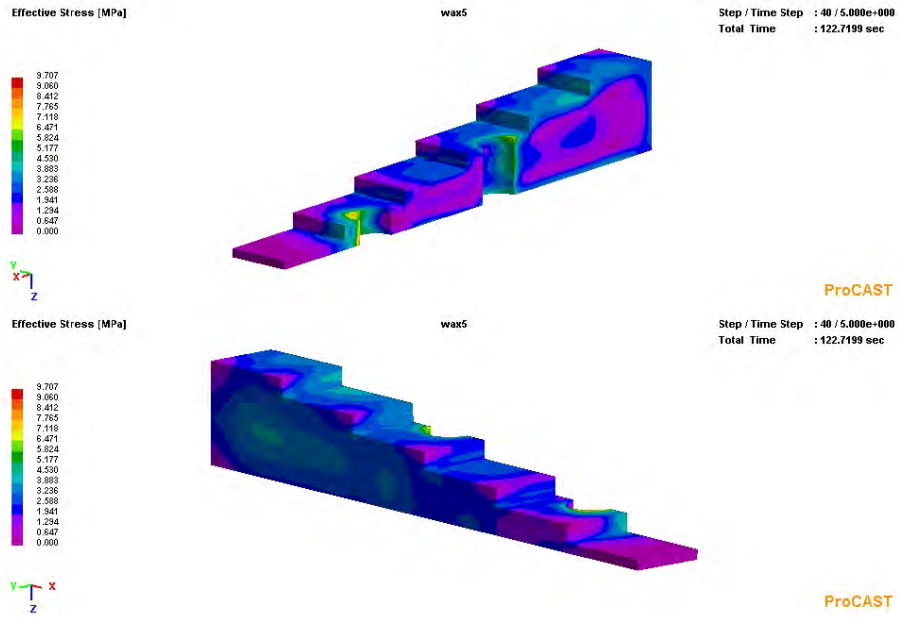


Figure 9 – Effective Stress After 2 Minutes

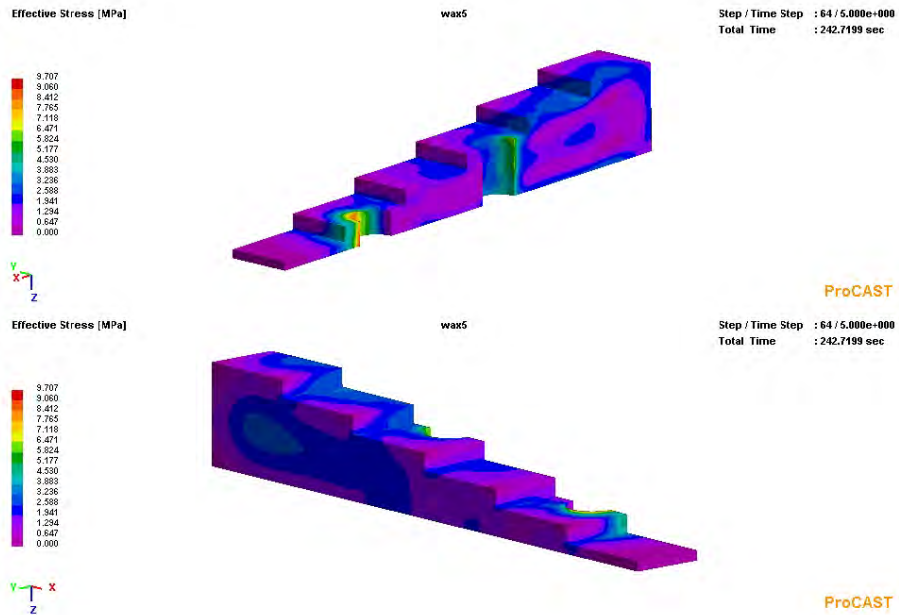


Figure 10 - Effective Stress After 4 Minutes

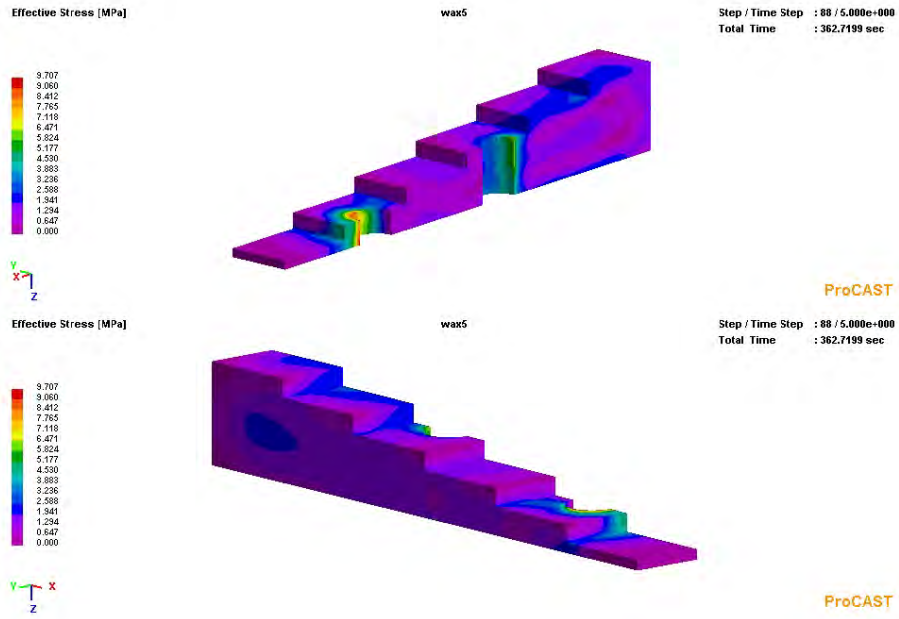


Figure 11 - Effective Stress After 6 Minutes

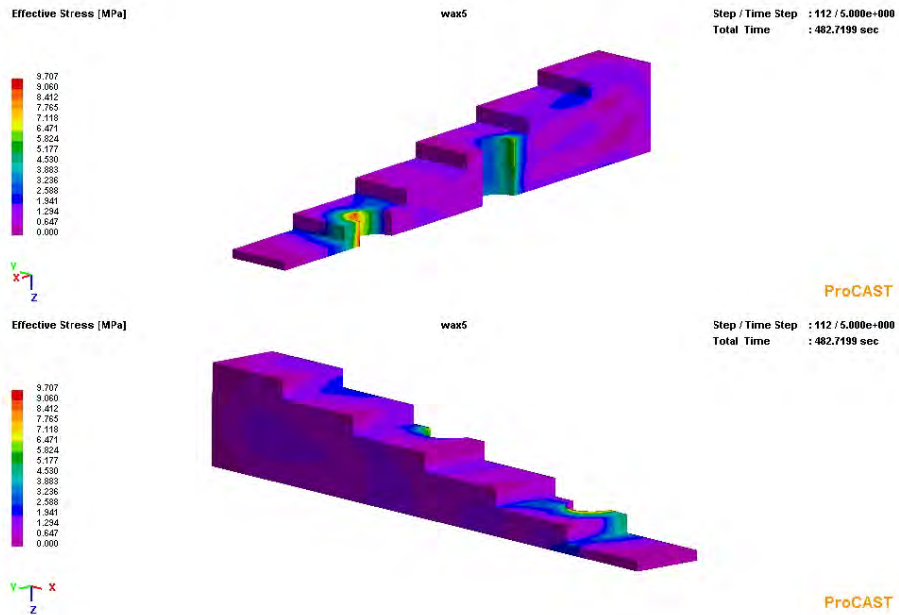


Figure 12 - Effective Stress After 8 Minutes

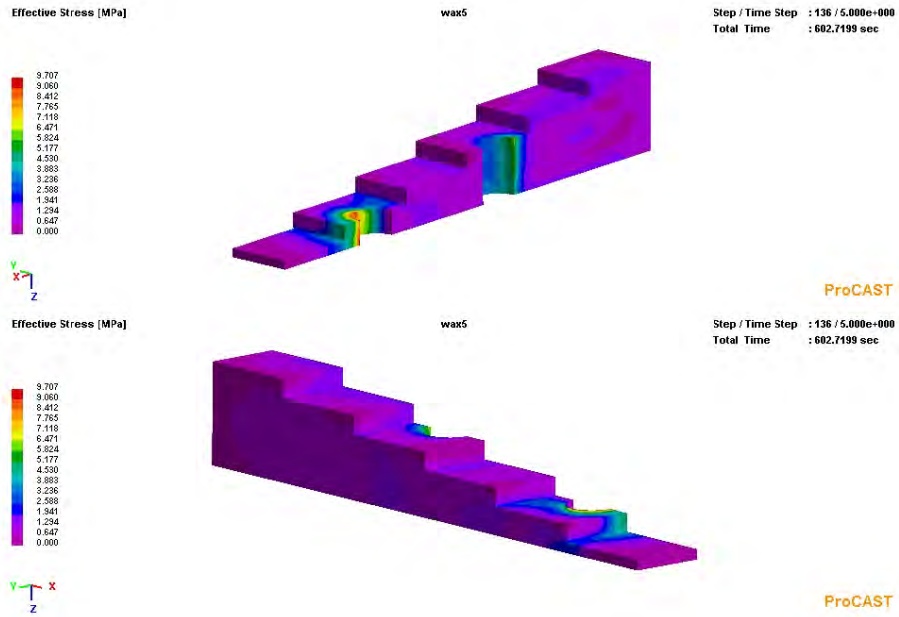


Figure 13 - Effective Stress After 10 Minutes

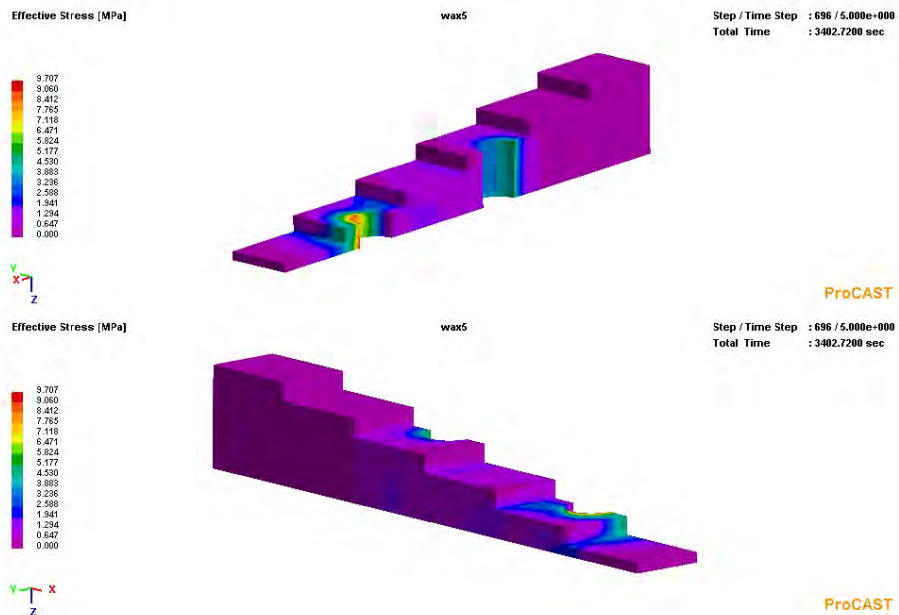


Figure 14 - Effective Stress – Final State

While the Effective, of Von Mises, Stresses provides a view of the net stress state in the wax, a Principal Stress 1 plot highlights the regions of tension in the part. It is possible that when the wax is removed from the tooling, these tension stresses could relax some amount due to the lack of constraint from the posts which create the holes in the wax. However, given that the maximum tension developed at any time in this model is only 18 MPa, it can be assumed that any stress relaxation will result in a minute amount of deformation. In this analysis, the final state of the wax does not assume this ejection and stress relief. Figures 15-20 present the evolution and final Principal 1 stress state in the wax step block.

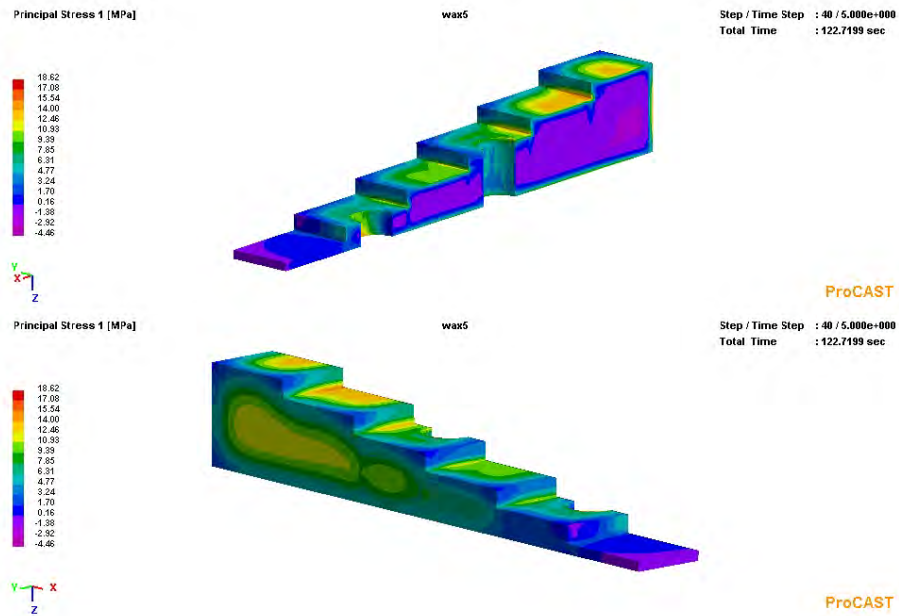


Figure 15 – Principal Stress 1 After 2 Minutes

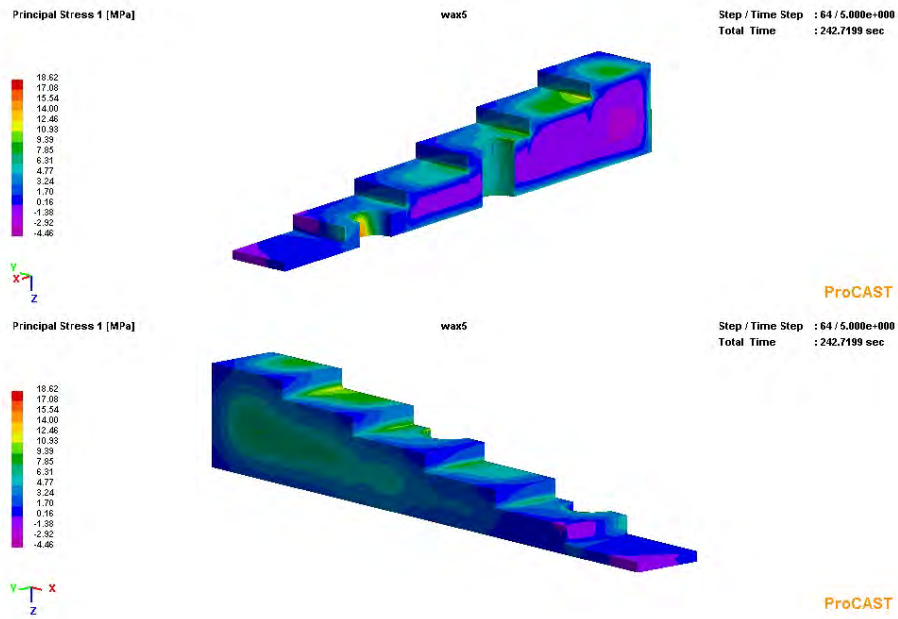


Figure 16 – Principal Stress 1 After 4 Minutes

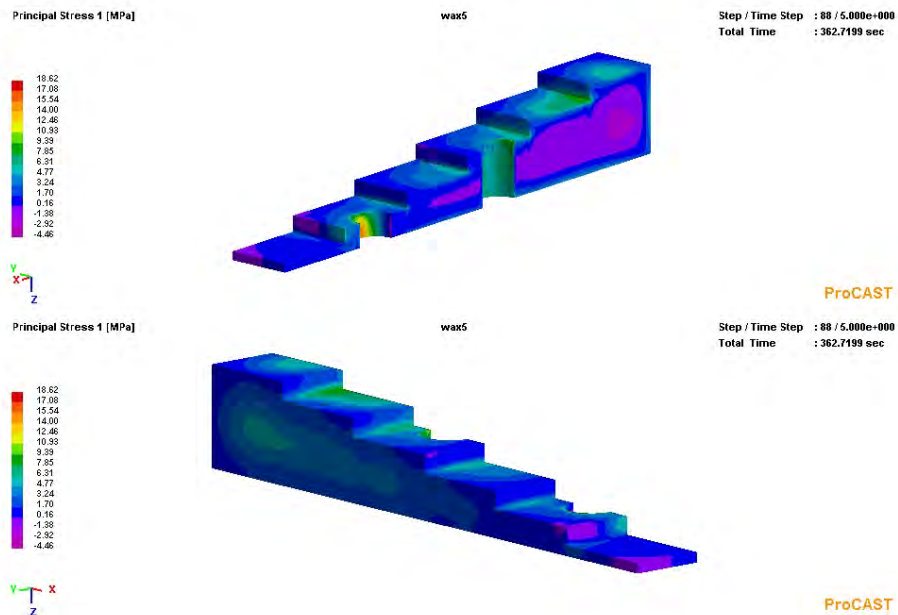


Figure 17 – Principal Stress 1 After 6 Minutes

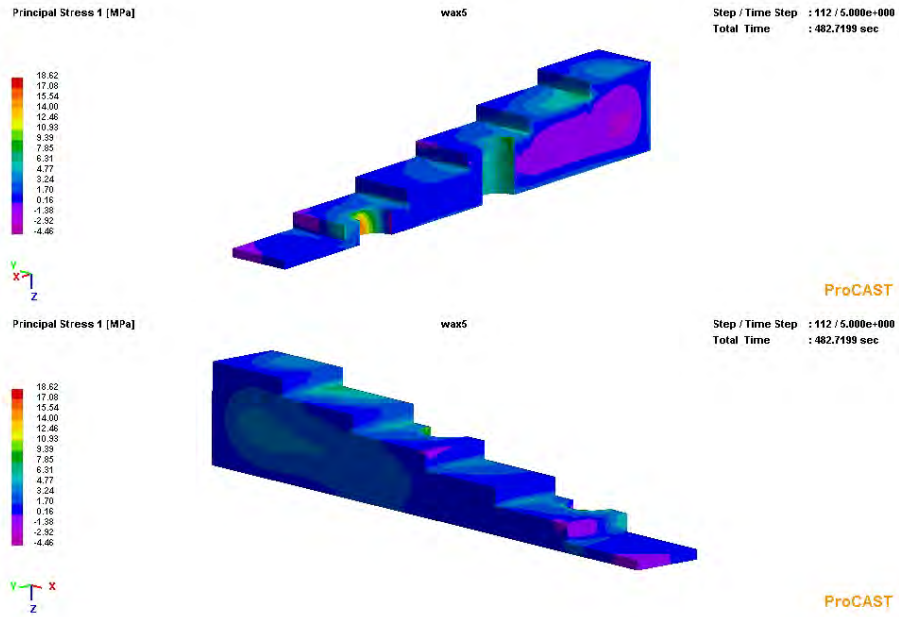


Figure 18 – Principal Stress 1 After 8 Minutes

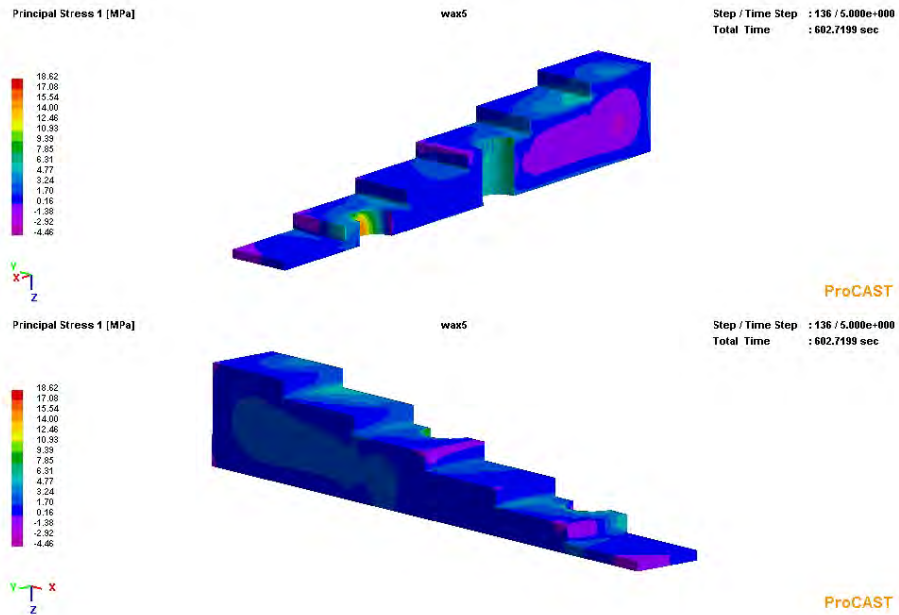


Figure 19 – Principal Stress 1 After 10 Minutes

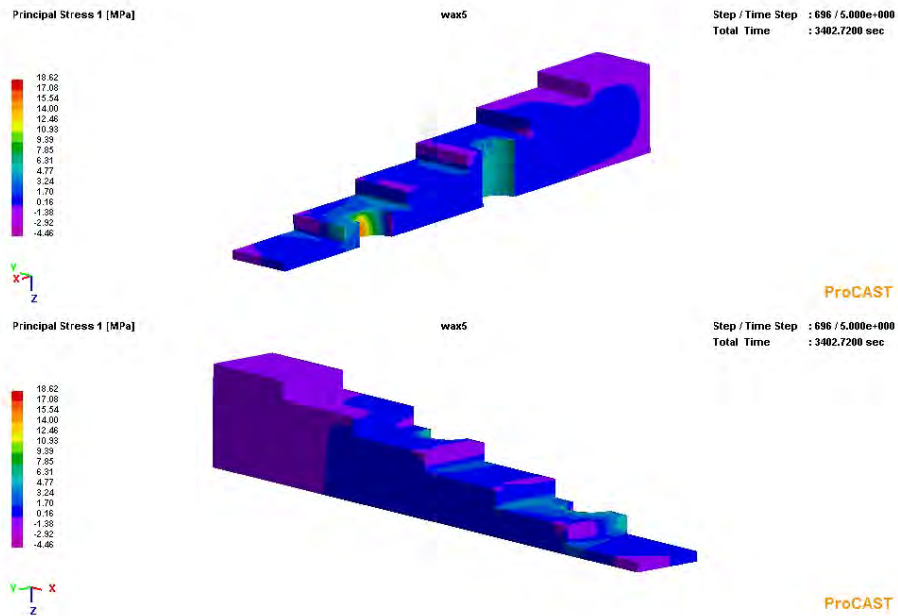


Figure 20 – Principal Stress 1 – Final State

Figures 21 and 22 display the mesh deformation, scaled by a factor of 10 to better visualize the deformation shape. In the top view (Figure 21), there are a few items of interest. In the vicinity of the left hole, there is a “bulge” or restriction from shrinking in the width (Y-direction) of the part. This is likely caused by the hole-forming post of the wax die. Near the right hole, significant shrink has attempted to occur, with the result being that the die post contact constraint has severely deformed the hole shape, and warped the corner of that thickness out beyond the side wall. Finally the thin section of the part has a significant taper along the width due to the free deformation at the end of the block versus the severe warping caused by the right hole.

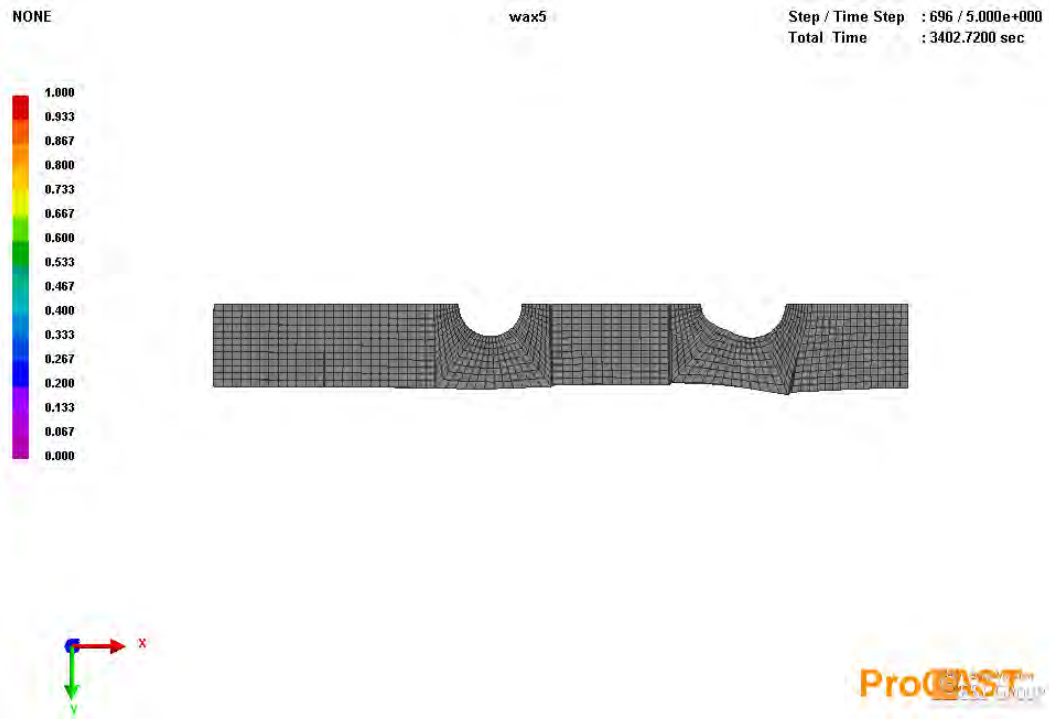


Figure 21 – Final Deformed Wax Part (Magnified 10x)

Not as much deformation is seen in the vertical thickness of the step block (Z-direction), as the part is free to shrink along all sections (Figure 22).

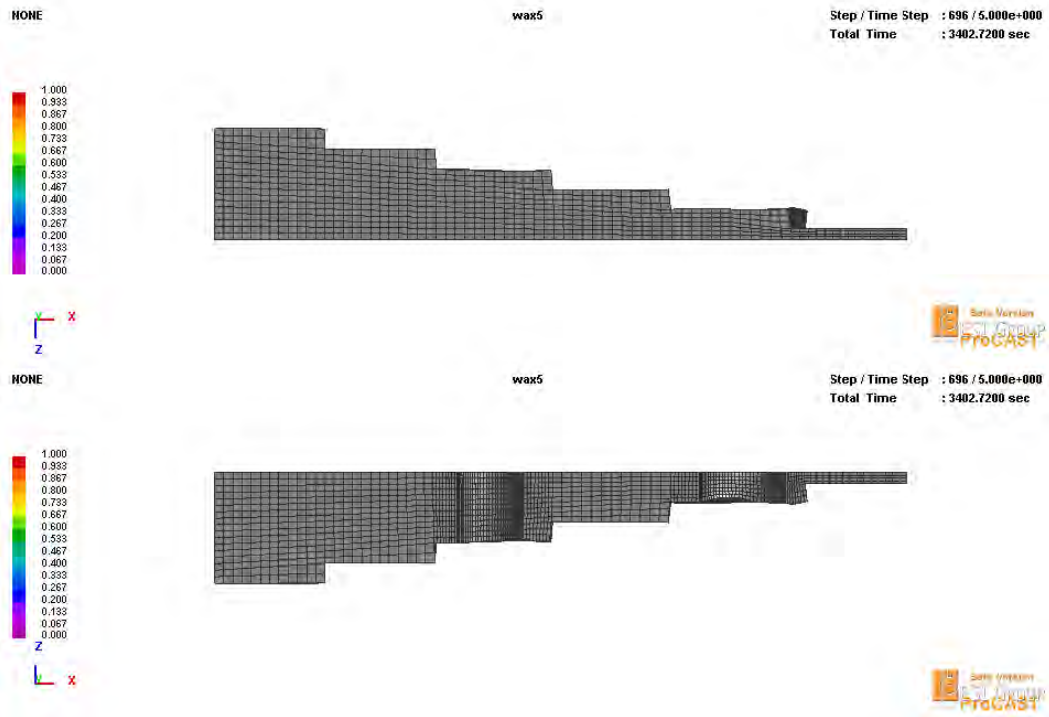


Figure 22 – Final Deformed Wax Part (Magnified 10x)

Lastly, the net deformation in each of the X-, Y- and Z-directions are shown in Figures 23-25.

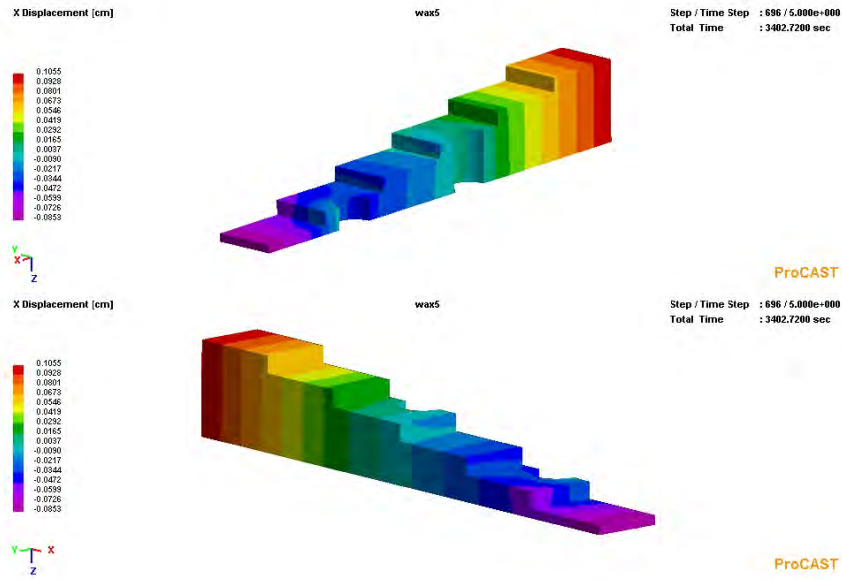


Figure 23 – X-Displacement (Values Relative to Original Position)

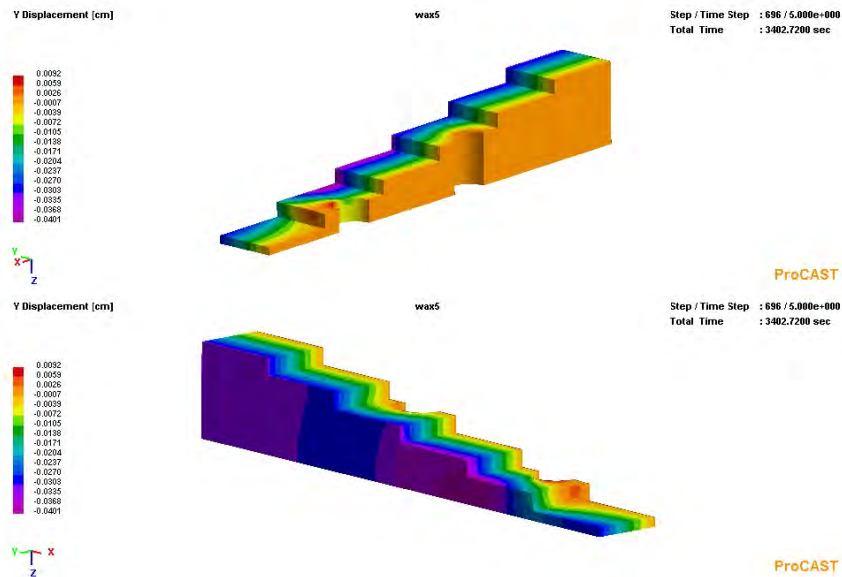


Figure 24 – Y- Displacement (Values Relative to Original Position)

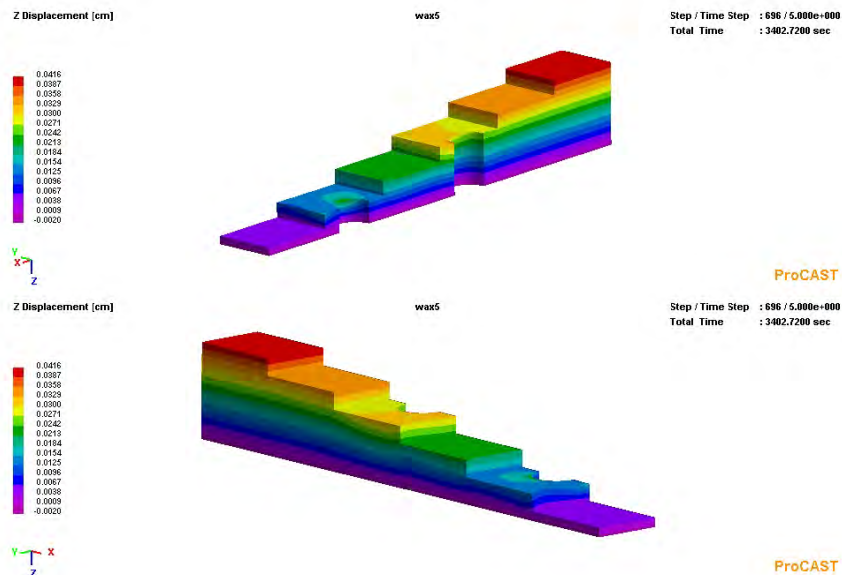


Figure 25 – Z-Displacement (Values Relative to Original Position)

6.1 Comparison of Analysis Results to Experimental Data

The first direction to be compared will be the length of the step block (X-direction). Figure 26 presents a graph plotting the experimentally measured length versus that determined by simulation. The data points in this direction were determined at the centerline of the block, 7 mm from the centerline and 14 mm from the centerline. The overall distance was taken from the left side of the block, where the thickest section is located, to the side face of each step, effectively measuring the length of each step. The points were selected to be at the same height (Z-direction) in the block. The “Shrinkage” value is the difference between original mold cavity distance minus the final wax shape distance at the same data point pairs. The experimental curves are plotted using the solid lines, while the ProCAST determined curves are represented by the dotted lines.

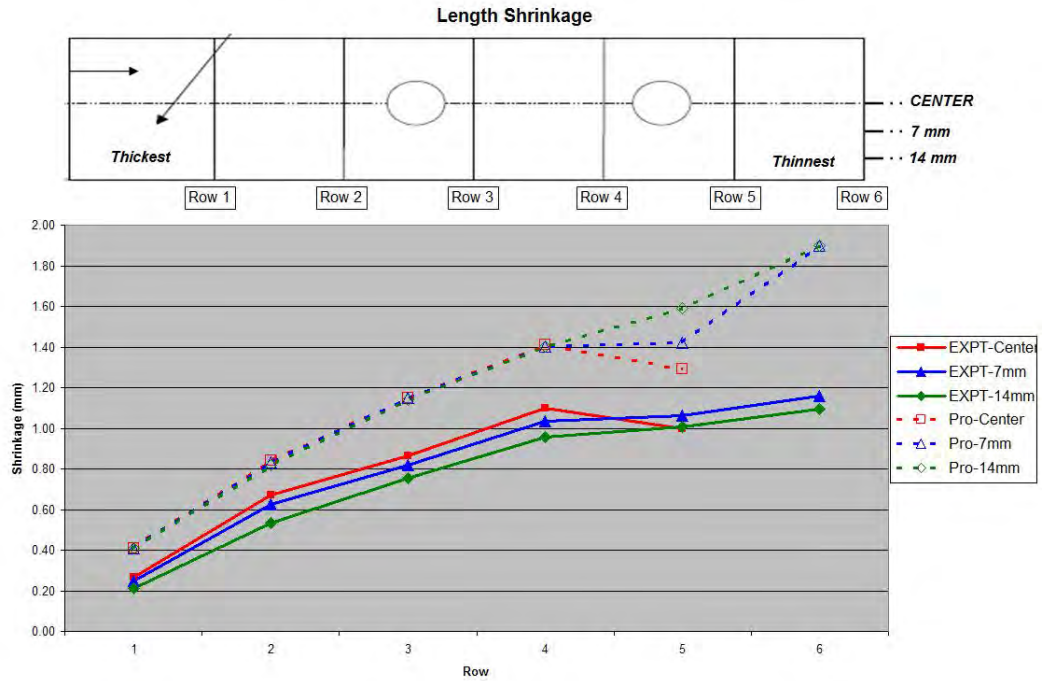


Figure 26 – Shrinkage Along Test Part Length (X-Direction)

The trend comparison between simulated and experimental results is quite good, with an apparent scaling factor variation with increasing distance from the left end. This error may be a result of improper thermal expansion data, which was supplied by the manufacturer and not validated. The error may be supplemented by the lack of intensification in the simulation. Wax intensification would continue to add wax into the cavity of the die until the wax is too cold to allow this additional filling. Therefore, intensification would help the wax maintain the cavity shape, especially near the point of injection, which is the thick section of this part. A sharp reduction in shrinkage in the center of block after the right side hole is also appropriately captured by simulation. The mold dimension at the center of row 6 was not provided, and thus not included in this graph.

Figure 27 shows the comparison of the results in the width of the part (Y-Direction). Each step was measured at the mid-height of the step on both sides of the wax. The experimental data is plotted in the blue curve, while the ProCAST results are shown in red. As done in the length direction, these wax width distances were compared to the mold cavity distances, where the difference is the net shrinkage of the wax. Also similar to the length results, the simulation shrink values are higher than the actual wax. Again, this may be a factor of improper thermal expansion coefficient and/or wax intensification.

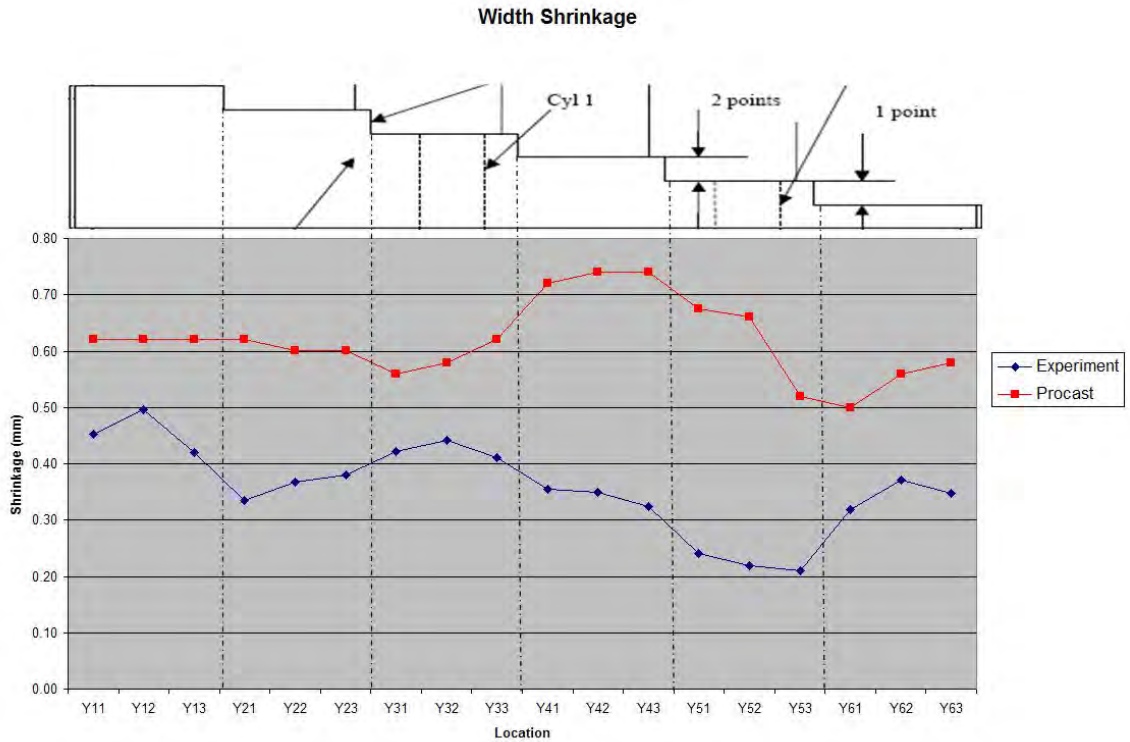


Figure 27 - Shrinkage Along Test Part Width (Y-Direction)

However, unlike the length comparison, the same trend is not seen between analysis and experimental results. Moving along the block from left to right, the thickest steps have the ability to freely shrink in the width, which is well noted in the ProCAST results with a nearly constant shrink amount. In the third step, where the left hole is located, the experimental results show a slight increase in shrink at the hole, while the simulation results show a slight decrease. Physically, a decrease makes more sense, as (1) the die steel forming the hole will prevent deformation, which leads to less shrink, and (2) there is less wax material in this section to generate shrinkage.

The fourth step, which is between holes is an interesting case in itself. This section will generally have free shrinking in the center, but will also be subject to the constraints at the holes. The part will want to shrink along the length, but cannot; therefore, tension will form between the holes, as seen in the Principal Stress 1 plots presented earlier. A section undergoing active tension or pulling from each end, as is the case with the hole constraints, will have a "necking" deformation, where the center of the section will become thinner due to the pulling forces. This phenomenon is seen in the ProCAST results, where there is an increase in shrink in this section. The experimental results do not show such an amount of shrinkage, which may be a result of stress relaxation after ejection.

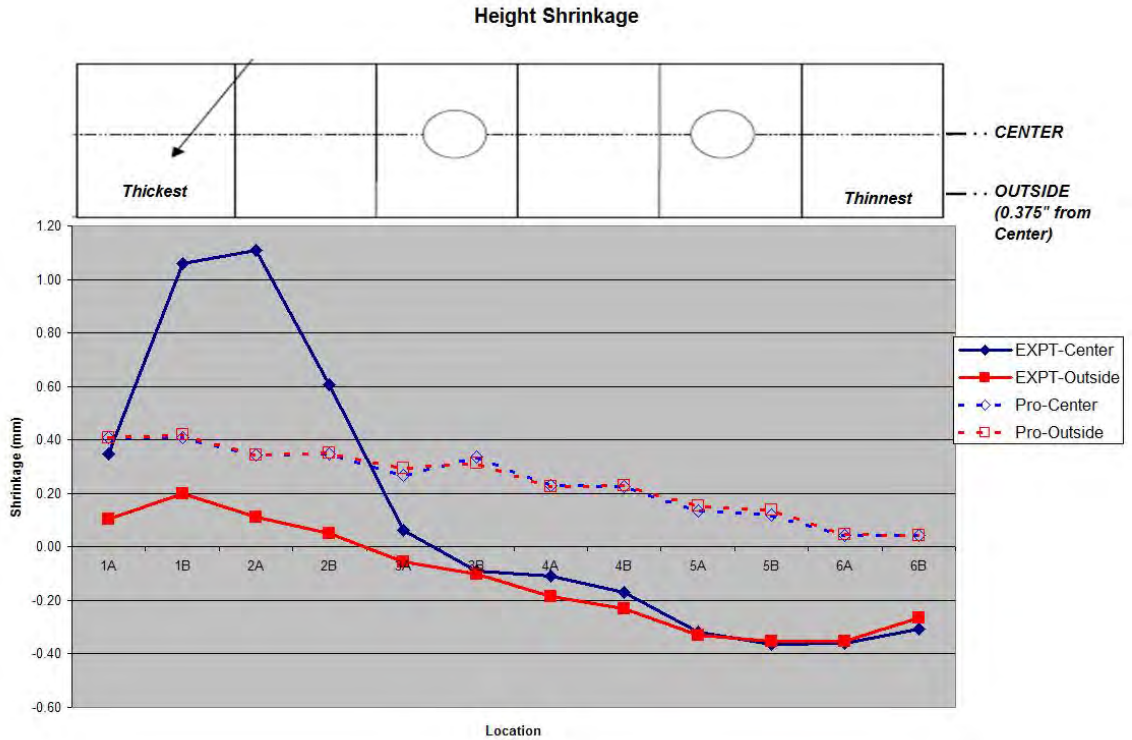


Figure 28 - Shrinkage Along Test Part Height (Z-Direction)

The final direction of comparison is in the height of each step of the wax shape. Data was collected at two points along the length of each step, at the $\frac{1}{4}$ and $\frac{3}{4}$ lengths of each step. These data points were repeated 0.375" (9.525 mm) from the centerline of the step block. Figure 28 presents the resultant data at these various locations. The solid curves are the experimental results, while the dotted curves are the ProCAST simulation results. The blue curves correspond to the results along the centerline, whereas the red curves show the off-center results.

As noted previously, there is no restriction to shrink deformation in this direction. There may be some influence via the hole constraints, but that contribution should be minimal. Therefore, the result trend should show an amount of shrink that is proportional to the die height of each step, where the net shrinkage is less with each step due to less material through the step thickness. Indeed, that trend is clearly seen in the ProCAST results, where each step has similar shrink values, and as the step size decreases, so too does the shrink amount. There are some small variations caused by the hole constraint influence, most notably at location 3B.

The experimental results present an entirely different scenario. In the thicker two steps, there is large disagreement between the shrinkage at the center of the wax versus the outer data point. This could be explained by a much slower cooling rate in the center of the face of the wax than at the edge. The analysis shows this variation in cooling rate, but it may be larger in reality than as simulated. This would cause the center of the face to sink into the center of the part. This theory would contradict any wax intensification effects.

Starting at the third step and continuing to the thin end of the part, the experimental results show a net expansion of wax. This result is simply inexplicable, and thus will not be discussed.

7. Benefits Assessment

This addition of this new modeling data was originally estimated to result in minor energy savings as compared to the entire Energy-SMARRT effort. However current (2011) annual energy saving estimates based on commercial introduction in 2011 (5% of market) and a market penetration of 50% by 2020 is 0.24 trillion BTU's/year and an estimated 2.4 trillion BTU's/year with 50% market penetration by 2020.

Along with these energy savings, reduction of scrap and improvement in casting yield will result in a reduction of the environmental emissions associated with the melting and pouring of the metal which will be saved as a result of this technology. The average annual estimate of CO₂ reduction per year through 2020 is 0.41 Million Metric Tons of Carbon Equivalent (MM TCE).

See Appendix A.

8. Commercialization

The results from the developments were incorporated into the commercial casting analysis software ProCAST, which is owned and maintained by ESI Group. ESI transferred the wax material property data into separate temperature-dependent thermophysical and mechanical property datasets and then consolidated the data into an easily viewable and modifiable user interface within the pre-processing application of the ProCAST suite (PreCAST).

9. Conclusion

In this project, ESI Group NA has completed the large vision of work in implementing a usable and accurate simulation tool for modeling the deformation of wax patterns during the solidification and cooling stages of wax manufacturing. Building upon previous work, the previously acquired material property data was converted into a form usable by the software and constitutive equations used to solve the various heat transfer and mechanical transient observed during the process. This data is easily viewable in the pre-processing graphical user interface (GUI) provided as part of the software package. Finally, an analysis was performed simulating the solidification and cooling of a test block which was also manufactured and measured. The results between analysis and reality compare very well, and the calculation appears to appropriately capture the physics of the scenario, thus validating its use to other waxes and geometries.

10. Recommendations

As outlined in the original scope of this effort, it was envisioned to include certain “filled” waxes in this project, and thus have those materials also available for use in the software. The same steps would be required to implement these waxes, those being experimental material property measurement, conversion and transferal into the software, and experimental validation. Current funding does not allow this effort, as the volume of material property data thought to have been acquired is actually insufficient. Additional funding provides for further material property data acquisition, testing, and building of the wax database for those interested in this technology.

References

1. Prediction of Wax Pattern Dimensions in Investment Casting; Sabau, A.S. and Viswanathan, S; Transactions of the American Foundry Society V 110 Paper No 02-103 P 733-746, 2002 (14 p)
2. Temperature Measurements in Wax Patterns and Wax-Die Interfacial Heat Transfer Coefficients in Investment Casting; Sabau, A.S. and Viswanathan, S.; Transactions of the American Foundry Society V 111 Paper No 03-026 P 463-472, 2003 (10 p)

3. Appendix A – Benefits Assessment Support Data

Estimated Investment Castings 2011-2020 (ICI)

Year	2011	2012	2013	2014	2015	2016	2017	2018	2019	2020
000 Tons	108	124	137	138	149	155	162	163	162	151

Scrap estimate: 7% per year (ICI)

Market Share: 5% in 2011. Full penetration of 50% by 2020. Estimated scrap reduction per year is 10% for foundries utilizing pattern prediction modeling software (AFS)

Estimated energy used per pound of investment casting: 8,518.94 MBBTUs/lb (IAC)

ICI: Investment Casting Institute

AFS: American Foundry Society

IAC: Industrial Assessment Centers